Kinetic Model for Separation of Particle Mixtures by Interfacial Partitioning

M. A. Hoeben, R. G. J. M. van der Lans, and L. A. M. van der Wielen
Kluyver Laboratory for Biotechnology, Delft University of Technology, Julianalaan 67, 2628 BC Delft, The Netherlands

G. Kwant
DSM Research, P.O. Box 18, 6160 MD Geleen, The Netherlands

DOI 10.1002/aic.10105
Published online in Wiley InterScience (www.interscience.wiley.com).

A mechanistic study is presented on the partition behavior of mixtures of particles in interfacial partitioning with liquid two-phase systems. A model is developed based on a mechanism of competitive adsorption of particles at the liquid-liquid interface. In this model, it is assumed that partitioning is the result of a dynamic process of continuous adsorption and desorption of particles at droplet interfaces. It is shown that under certain conditions such a process can be described by means of Langmuir-type adsorption isotherms. The model is tested with partition data of mixtures of ampicillin and phenylglycine crystals in a water/n-pentane system, which leads to a reasonable quantitative description. The results indicate that for this particular system, adsorption of crystals at the interface occurs up to amounts that are needed for a monolayer coverage. In case larger amounts of crystals are present, partitioning of particles is subject to a competition for the available interfacial area. In such a case, the kinetics of adsorption and desorption of the particles to the interface seem to differ from a situation where the interface is partly uncovered. © 2004 American Institute of Chemical Engineers *AIChE J,* 50: 1156–1168, 2004
Keywords: particle recovery, interfacial partitioning, crystals, Langmuir-isotherm, adsorption

Introduction

Many products in biotechnology are solids. Current developments in fields such as genetic engineering and biocatalysis result in the efficient production of bioproducts in ever increasing concentrations. As a consequence, products are likely to be produced above the solubility more frequently in the future, which implies that purification of products in solid form is becoming an issue of increasing importance. Solid bioproducts might be obtained in the form of precipitates, crystals or more complex structures such as virus-like particles. The sizes of such bioparticles may vary from several tens of nanometers to well above 100 μm. A specific group within this whole spectrum of products that is recently gaining more attention, are products that consist of self-assembling biopolymers such as DNA, RNA, and viruses. Here, even a single molecule can feature the properties of a particle (Kimura et al., 1996). Purification of these compounds is an essential step in the production of gene therapy products, and will as such provide future challenges as developments in this area progress.

In general, the purification of bioparticles involves the separation of the product from reaction mixtures containing suspended materials, such as insoluble substrates, byproducts, as well as cells and cellular fragments. If the product particles differ little in size and density from those they have to be separated from, the conventional techniques such as centrifugation or filtration are not effective. This problem can, for example, occur in processes that involve solid-to-solid bioca-

Correspondence concerning this article should be addressed to L. A. M. van der Wielen at L.A.M.vanderwielen@tnw.tudelft.nl.

talysis, such as the enzymatic production of peptides (Halling et al., 1995). In these cases, the conventional approach is to recover the product by dissolution, followed by molecular separation, such as extraction or adsorption and selective (re-) crystallization. However, if direct particle-particle separation would be possible, the number of process steps could be reduced, resulting in a reduction of process costs. Another example where solid-solid separation may be beneficial is the production of recombinant proteins. When expression occurs intracellularly, the product may be obtained in the form of inclusion bodies, which can be crystals or precipitates with sizes in the same range as the cells. Separation of inclusion bodies from cell debris can sometimes be achieved by centrifugation. However, in some cases this can be a complicated matter because of overlapping size distributions (Wong et al., 1996), or the procedures used on lab scale, such as density gradient centrifugation are not suitable for large scale production (Liu et al., 2000). These examples indicate the need for new separation methods that are suitable for particles with similar sizes and densities.

As an alternative for centrifugation, Walker and Lyddiatt (1999) reported on the separation of inclusion bodies from cell debris in homogenates of *E. coli* by means of aqueous two-phase partitioning. They showed that at optimal values of pH and additional salt (NaCl) concentration, 87% of the inclusion bodies could be recovered from the bottom phase, whereas the cell debris accumulated in an interphase between the salt and polymer rich phases. The efficiency of the method proved to be much higher than with conventional centrifugation. Although density gradient centrifugation turned out to give even better results, this technique is not feasible at a larger scale because of low process throughput and extended process times. Andrews et al. (1995) reported on the application of aqueous two-phase systems for the purification of virus-like particles from a yeast cell homogenate. They propose two strategies for the purification process among which there is one where partitioning of the virus-like particles to an interphase is involved. Also in this case, the authors stress that the presence of an additional salt can have a large impact on the partition behavior of the particles. Purification of solid bioproducts in liquid two-phase systems by partitioning to an interphase was described earlier by Pike and Dennison (1989). In their work they report that proteins can be precipitated from solution into a third phase positioned at the interface in a water/t-butanol system. This process occurs under the influence of ammonium sulfate that is added to the water phase and t-butanol molecules that were believed to bind to the proteins giving them an increased buoyancy. The influence of several parameters was investigated, such as pH, temperature, and salt concentration, and the large potential of the method was shown by experiments with several proteins. In more recent work Dennison and Lovrien (1997) further elaborate on this method which they refer to as three-phase partitioning. Special attention is paid to the importance of electrostatic interactions between the proteins and the ions of the added salt.

In all the earlier studies, the formation of a particles-containing interphase was reported. In previous work Jauregi et al. (2002) presented a study on properties of interphase layers that are formed in two-phase systems containing ampicillin, phenylglycine, and glycine crystals. It was found that the interphase had an emulsion-like character. It was shown that the interphase layers can have high capacities indicating that interfacial partitioning has a potential as a large scale separation technique. This potential was demonstrated in a second article where it was shown that phenylglycine and ampicillin crystals could be successfully separated by interfacial partitioning in water/butanol and water/hexanol systems (Jauregi et al., 2001). The sizes and densities of the crystals used were in the same range, which underlines that interfacial partitioning can be a useful alternative when separation by centrifugation or filtration is problematic. The concept of the emulsion-like character stated in the previous article was further elaborated. It was stressed that the crystals promote the formation of a solid-stabilized emulsion and that the properties of the interphase are determined by the polarities of the crystals.

The fact that particles can stabilize emulsions was first recognized by Pickering (1907) who noticed that colloidal particles that are wetted more by water than by oil can act as emulsifying agents for oil-in-water emulsions. Thereafter, numerous studies on this subject have followed (Tambe and Sharma, 1994; Binks and Lumsdon, (1999, 2000a,b,c,d); Ashby and Binks, 2000). Stabilization of emulsions takes place through adsorption of the particles at the interfaces of the droplets of the dispersed phase. The adsorbed particles form a steric barrier, which prevents coalescence of the droplets. In general it is recognized that particles tend to stabilize emulsions where the continuous phase is the phase by which they are preferently wetted. Partitioning of clay particles between droplet interfaces and bulk liquid phase in solid-stabilized oil-water emulsions was investigated by Yan and Masliyah (1994, 1995). They propose that distribution of particles between liquid-liquid interface and bulk liquid phase is the result of a thermodynamic equilibrium. Their experimental data can be well described with adsorption isotherms allowing for multilayer coverage. In an earlier study, Levine et al. (1989a,b) treated the partitioning of small silica particles between the continuous water phase and interface in solid-stabilized water/toluene emulsions. Their analysis makes clear that the particles are very strongly adsorbed at the interface. Repulsive interactions between neighboring particles that reside at the interface (that is, electric double layer and short-range solvation and solid elastic forces, as well as capillary interaction) turn out to be far too low to account for a thermodynamic equilibrium between the adsorbed and desorbed state. They propose that the partitioning of particles between the interface and bulk liquid phase in situations where the droplets are not entirely covered with particles should be explained on the basis of drop dynamics.

It is clear that the combined literature on particle-stabilized emulsions contains important information about phenomena that occur in interfacial partitioning processes. As yet, however, the link between these two fields of research has barely gained any attention. As such, the description of interfacial partitioning until now has been rather qualitative in nature. It seems obvious that adoption of the concepts that are treated in colloid science can help in the development of a quantitative description of interfacial partitioning.

This article deals with the development of a Langmuir-type mechanistic model for the quantitative description of interfacial partitioning of particle mixtures. The model presented here is based on the hypothesis of the formation of an emulsion-like interphase layer as presented earlier by Jauregi et al. (2001,

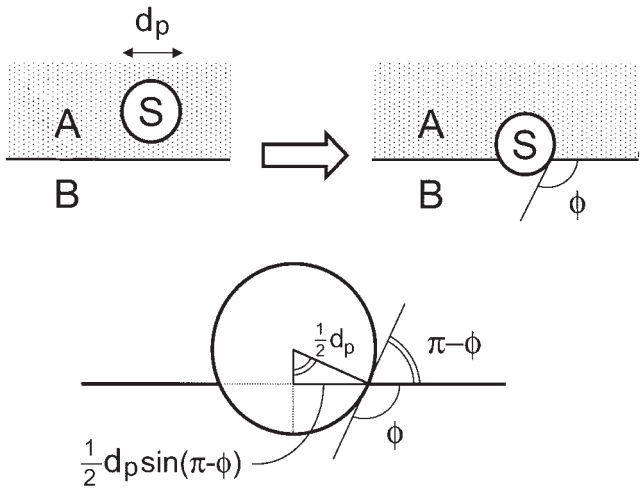

Figure 1. Adsorption process of a spherical particle at the interface between two liquids A and B.

2002). Evaluation will be performed on the basis of experimental data on the separation of ampicillin and phenylglycine crystals. The separation of these two crystals is an interesting case study, because it represents an existing industrial problem in the semisynthetic production of ampicillin (Bruggink et al., 1998). It will be shown that interfacial partitioning can be used to separate ampicillin and phenylglycine crystals with different liquid two-phase systems, and that their partition behavior can be described with a Langmuir-type mechanistic model.

Theory

Adsorption of particles at interfaces

Adsorption of particles at liquid-liquid interfaces reduces the liquid-liquid interfacial area. This causes a reduction in the Gibbs energy relative to a suspension of the particles in one of the bulk phases with a term equal to the interfacial tension times the interfacial area occupied by the particle. In case a spherical particle with diameter d_p adsorbs (see Figure 1), the reduction in interfacial area between the liquids is

$$-\Delta A_{AB} = \pi(\tfrac{1}{2} d_p \sin(\pi - \phi))^2 = \pi(\tfrac{1}{2} d_p \sin \phi)^2 = \tfrac{1}{4} \pi d_p^2 \sin^2 \phi \quad (1)$$

where ϕ is the contact angle between the liquid-liquid interface and the solid-liquid interface measured through liquid B.

In case gravity can be neglected and the liquid-liquid interface is planar up to the contact line with the particle, the change in Gibbs energy upon adsorption of the particle at the liquid-liquid interface from a suspension in liquid A is equal to (Binks and Lumsdon, 2000a)

$$\Delta E_{ads} = \tfrac{1}{2} \pi d_p^2 (1 + \cos \phi) \gamma_{BS} + \tfrac{1}{2} \pi d_p^2 (1 - \cos \phi) \gamma_{AS} - \pi d_p^2 \gamma_{AS} + \Delta A_{AB} \gamma_{AB} = \tfrac{1}{2} \pi d_p^2 (1 + \cos \phi)(\gamma_{BS} - \gamma_{AS}) - \gamma_{AB} \cdot \tfrac{1}{4} \pi d_p^2 \sin^2 \phi \quad (2)$$

where γ_{AS}, γ_{BS} and γ_{AB} are the interfacial tensions at the solid-liquid A, solid-liquid B, and liquid A-liquid B interface, respectively (N/m).

If the term $\gamma_{AB} \cdot (1/4) \pi d_p{}^2 \sin^2 \phi$ is sufficiently large, ΔE_{ads} will be negative and the particle will find itself in an energetically stable position at the interface. As the system will strive for minimization of Gibbs energy, the particle will be positioned such that the contact angle ϕ will have a value ϕ_{eq} at which ΔE_{ads} is minimal. Differentiating 2 with respect to ϕ and equating to zero gives

$$0 = \left[\frac{d(\Delta E_{ads})}{d\phi} \right]_{\phi = \phi_{eq}} = -\frac{1}{2} \pi d_p^2 (\gamma_{BS} - \gamma_{AS}) \sin \phi_{eq} - \gamma_{AB} \frac{1}{4} \pi d_p^2 \cdot 2 \sin \phi_{eq} \cos \phi_{eq} = \frac{1}{2} \pi d_p^2 \sin \phi_{eq} \times (\gamma_{AS} - \gamma_{BS} - \gamma_{AB} \cos \phi_{eq}) \quad (3)$$

Given that $0 < \phi_{eq} < \pi$ (and, thus, $\sin(\phi_{eq}) \neq 0$), this implies that

$$\gamma_{AS} - \gamma_{BS} - \gamma_{AB} \cos \phi_{eq} = 0 \rightarrow \gamma_{AS} - \gamma_{BS} = \gamma_{AB} \cos \phi_{eq} \quad (4)$$

which is the well-known Young equation. Substituting 4 into 2 gives

$$\Delta E_{ads} = -\tfrac{1}{2} \pi d_p^2 (1 + \cos \phi_{eq}) \gamma_{AB} \cos \phi_{eq} - \tfrac{1}{4} \gamma_{AB} \pi d_p^2 \sin^2 \phi_{eq} \quad (5)$$

which can be rearranged to

$$\Delta E_{ads} = -\tfrac{1}{4} \pi d_p^2 \gamma_{AB} (1 + \cos \phi_{eq})^2 \quad (6)$$

This equation shows that a high interfacial tension γ_{AB} between liquids A and B can lead to a large negative value of ΔE_{ads}, which means that the particle might be firmly attached to the interface. Whether or not the particle will remain positioned at the interface depends on the magnitude of other forces. If a density difference exists between the particle and the surrounding liquid, a net force F_g, arising from the difference between gravity and buoyancy, applies to the particle. In case the density difference between the two liquids is small compared to the density difference between the liquids and the particle F_g can be approximated by

$$F_g = \tfrac{1}{6} \pi d_p^3 (\rho_p - \bar{\rho}_l) g \quad (7)$$

where ρ_p is the density of the particle (kg/m^3), $\bar{\rho}$ is the average density of liquids A and B (kg/m^3) and g is the gravitational acceleration (m/s^2).

If F_g is large enough, a particle that is positioned at the interface will be pulled from the interface into the bulk liquid. In other words, the change in gravitational energy upon movement of the particle in the direction of F_g is large enough to compensate for the increase in energy with a value of ΔE_{ads} which occurs upon desorption of the particle from the interface.

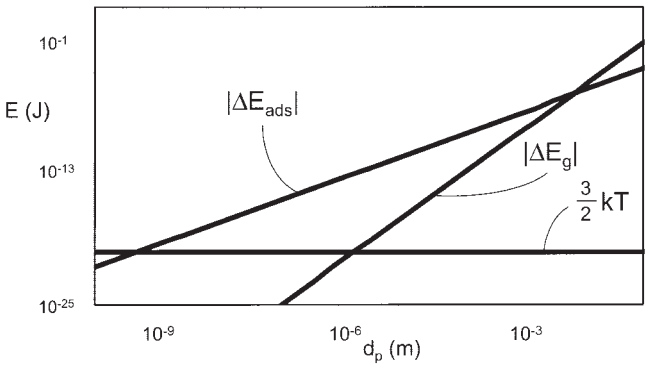

Figure 2. The absolute values of ΔE_g and ΔE_{ads} for the removal of a spherical particle from a horizontal interface plotted vs. the diameter of the particle.

ΔE_g is defined as the change in gravitational energy of the whole system. ΔE_{ads} is defined as the change in total interfacial energy of the system. The difference between the density of the particle and the average density of the liquids (ρ_p - $\bar{\rho}$) is 200 kg/m^3, the interfacial tensions between the two liquids γ_{AB} is 30 mN/m, the three-phase contact angle ϕ_{eq} is 90° and the absolute temperature T = 298 K.

Removal of the particle from the interface implies a total displacement of the particle of about half its diameter. The change in gravitational energy of the system associated with this displacement is equal to

$$\Delta E_g = \pm F_g \cdot \tfrac{1}{2} d_p = \pm \tfrac{1}{12} \pi d_p^3 (\rho_p - \bar{\rho}_l) g \qquad (8)$$

where the sign of ΔE_g is negative if the particle moves in the direction of F_g and positive if it moves in the opposite direction. In Figure 2, $|\Delta E_g|$, which is calculated according to Eq. 8, and $|\Delta E_{ads}|$, which is calculated according to Eq. 6, are plotted vs. the particle diameter for $(\rho_p - \bar{\rho})$ = 200 kg/m^3, γ_{AB} = 30 mN/m and ϕ_{eq} = 90°. The values of $(\rho_p - \bar{\rho})$, γ_{AB} and ϕ_{eq} are typical for silica particles with a hydrophobic coating at a water-toluene interface. Figure 2 shows that for this particular system $|\Delta E_g|$ starts to exceed $|\Delta E_{ads}|$ for particles with a diameter of about 1 mm. This means that for diameters smaller than 1 mm the resultant of gravity and buoyancy is too small to remove the particle from the interface. In this case, the most stable position is at the interface. However, for very small diameters this might no longer hold, because of the increasing importance of Brownian motion. The thermal energy which causes particles to display Brownian motion is independent of the diameter and equal to (3/2)kT. As can be seen in Figure 2, $|\Delta E_{ads}|$ only starts to become of the same order as (3/2)kT for diameters as small as 1 nm. This means that spontaneous desorption from the interface is only likely to occur for particles with molecular dimensions. As a result it appears that the size range of particles, which are likely to stay adsorbed at the interface once they arrive there, is rather wide, stretching from 1 nm to about 1 mm. Therefore, it seems that for most common particles found in bioprocesses, interfacial adsorption can be generally applicable, provided that interfacial adsorption is not accompanied by undesired by-effects, such as degradation. Once adsorbed at the interface, the particle might be trapped in a deep energy well, because ΔE_{ads} can outrange both ΔE_g and the thermal energy by several orders of magnitude.

Interfacial partitioning model

Selective interfacial partitioning can be established by contacting a particle mixture with a liquid-liquid system. Agitation will result in the creation of an emulsion, and after mixing is stopped, an emulsion layer is formed as a layer between top and bottom liquid phases, the so-called interphase (Jauregi et al., 2001). Part of the particles will end up in this interphase layer, whereas the remainder will be present in the bulk liquid phases. The particles that are present in the bulk bottom phase can be collected as a sediment, given that their density is higher than the density of the bottom phase. To enable the separation of different particles, the composition of the particle mixture that ends up in the interphase layer should differ from the composition of the mixture in the bulk liquid phases. The liquid-liquid system used for the operation should be chosen carefully to promote this difference. The mechanism of interfacial partitioning is not entirely unraveled yet, however, in this work we assume that partitioning of the particles occurs exclusively during the agitation step. The proposed mechanism is shown in Figure 3 and is assumed to be the result of a dynamic process where particles distribute between the continuous liquid phase and the interfaces of droplets. The particles that adsorb at the droplets will end up in the interphase. For reasons of simplicity, it is assumed that partitioning of particles into the dispersed phase does not occur. This assumption can only hold if the affinity of the particles for the dispersed phase is very small compared to the affinity for the continuous phase. (N.B.: Even when the affinity for the dispersed phase is very small, interfacial adsorption will often still occur. Only at very high aversion for the dispersed phase, the adsorption energy can

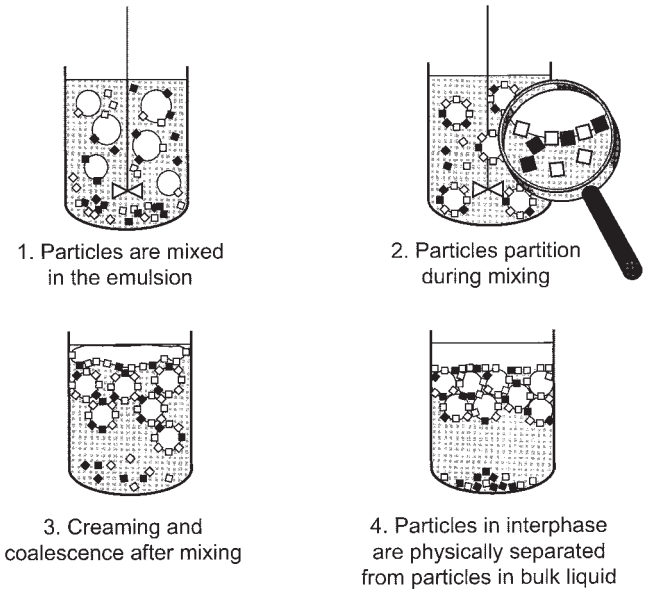

Figure 3. Hypothetical mechanism for the separation of two particles by interfacial partitioning.

Part of the particles adsorbs at the droplet interfaces, leading to a (partly) Pickering-stabilized emulsion.

become positive, in which case interfacial adsorption will not occur.)

During agitation, collisions will occur between particles and drops of the dispersed phase. If the energy associated with the collision is sufficient to cause drainage of the liquid film between drop and particle, contact occurs and the particle adsorbs. As a first approximation, we will assume that the number of effective collisions per unit of time and volume r_{ads} is proportional to the concentration of particles in the continuous liquid phase, and the interfacial area available for adsorption. For a system that contains two types of particles A and B, we can then write

$$r_{ads,A} = \frac{k_{ads,A} c_A A_{tot} (1 - \theta_A - \theta_B)}{V} \tag{9a}$$

$$r_{ads,B} = \frac{k_{ads,B} c_B A_{tot} (1 - \theta_A - \theta_B)}{V} \tag{9b}$$

where $k_{ads,A}$ and $k_{ads,B}$ are adsorption rate constants for particles A and B (m/s), c_A and c_B are the number of particles A and B in the continuous liquid phase per volume (m^{-3}), A_{tot} is the total droplet interfacial area (m^2), and V is the total volume of continuous phase (m^3), θ_A and θ_B are the fractions of the drop area covered with particles A and B, respectively. The definitions of θ_A and θ_B read

$$\theta_A = \frac{n_{A,i} \cdot a_A}{A_{tot}} \tag{10a}$$

$$\theta_B = \frac{n_{B,i} \cdot a_B}{A_{tot}} \tag{10b}$$

where $n_{A,i}$ and $n_{B,i}$ are the total numbers of particles A and B on the entire droplet interface, and a_A and a_B are the interfacial areas that a single particle effectively occupies (m^2).

It is obvious that the mixing conditions play an essential role in the adsorption process. Parameters, such as the power input and the dimensions of the stirrer, will therefore have an influence on the value of the adsorption rate constant k_{ads}. In a more extensive treatment similar to the adsorption of solid particles to liquid-gas interfaces (Schulze, 1984), k_{ads} can be split up into different terms. The adsorption rate constant k_{ads} can then be regarded as the product of a collision rate constant k_{col}, indicating the frequency of collision events between particles and droplets (m/s), and efficiency terms describing the probability that a collision leads to interfacial adsorption of the particle

$$k_{ads} = k_{col} \cdot P_{hyd} \cdot P_{int} \cdot P_{TPC} \tag{11}$$

where P_{hyd} = the hydrodynamic capture probability, (that is, the probability that the particle actually reaches the interface, given the hydrodynamic conditions), P_{int} = the probability that the thin liquid film between interface and particle will rupture and P_{TPC} = the probability of a successful three-phase contact formation.

P_{hyd} is entirely determined by hydrodynamics. P_{int} and P_{TPC}, however, are dependent on interfacial forces. The probability of rupture of the liquid film P_{int} depends on the magnitude of the forces that exist between the solid and the liquid that is not in contact with the solid. If the net resultant of these forces is attractive (over a certain range), spontaneous rupture of the film can occur. In this case P_{int} is nonzero.

The forces that govern the process of film rupture are the result of Van der Waals interactions, electrostatic interactions between the liquid-liquid interface and the liquid-solid interface and, thirdly, structural forces. The same interactions will play a dominant role in the establishment of the contact angle ϕ_{eq}. Therefore, P_{int} has a distinct relation with the interfacial adsorption energy ΔE_{ads}.

The same holds for the probability of three-phase contact formation P_{TPC}. That is, the energy, needed to move the three-phase contact line toward the equilibrium position, is in part determined by exactly the same interactions that define ΔE_{ads}. Therefore, in general terms, it can be stressed that a large negative value of ΔE_{ads} is likely to be accompanied with high values of P_{int} and P_{TPC} which induce an increase in $k_{ads.}$

Once the particles are adsorbed at the interface, they can be trapped in a deep energy well. There is, however, reason to assume that displacement of particles from the interface into the liquid can still occur. This is supported by experimental data of Levine and coworkers (1989a,b) who showed that notwithstanding a large, negative adsorption energy, partitioning of particles between bulk liquid and liquid-liquid interface during the mixing of an emulsion can still occur. Their analysis makes clear that it is not likely that this is because of the establishment of a thermodynamic equilibrium. According to the authors, the explanation for this has to be sought in the dynamics of droplet formation. In their view, the presence of particles in the liquid bulk phase is a consequence of the continuous breakup and coalescence of droplets during the mixing process. Indeed, coalescence of droplets is a fierce process and leads to the reduction of the interfacial area and can consequently lead to the release of adsorbed particles from the interface. If we assume that the number of desorption events per unit of time $r_{des,A}$ ($r_{des,B}$) is proportional to the fraction of the interface covered by particles A (B) we can write

$$r_{des,A} = k_{des,A} \frac{A_{tot}}{V} \theta_A \tag{12a}$$

$$r_{des,B} = k_{des,B} \frac{A_{tot}}{V} \theta_B \tag{12b}$$

where $k_{des,A}$ ($k_{des,B}$) is a desorption rate constant for particles A (B) ($m^{-2}s^{-1}$). Similar to the adsorption rate constant, k_{des} can be further split up into a term k_{freq}, accommodating the frequency of events that can lead to desorption, and a term P_{des} representing the probability that actual desorption occurs

$$k_{des} = k_{freq} \cdot P_{des} \tag{13}$$

The frequency term k_{freq} concerns all events that can displace particles from the interface. As mentioned previously, coalescence of two (partly) covered drops is one of these. Other

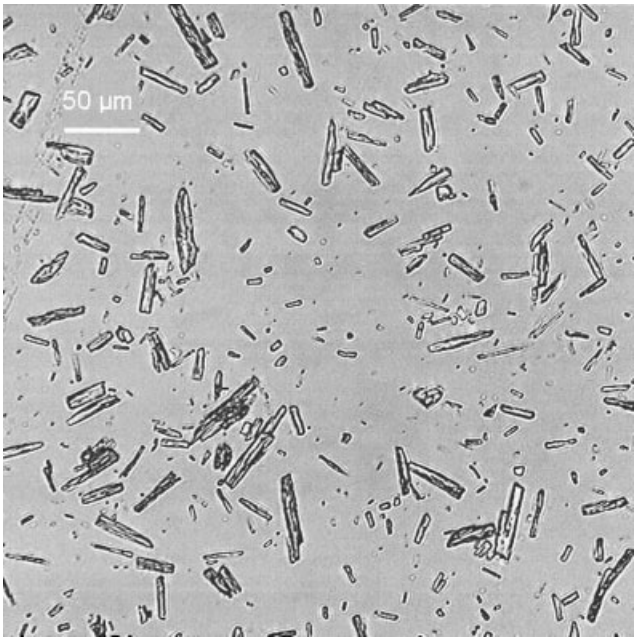

Figure 4. Microscopic image of the ampicillin trihydrate crystals used in the experiments.

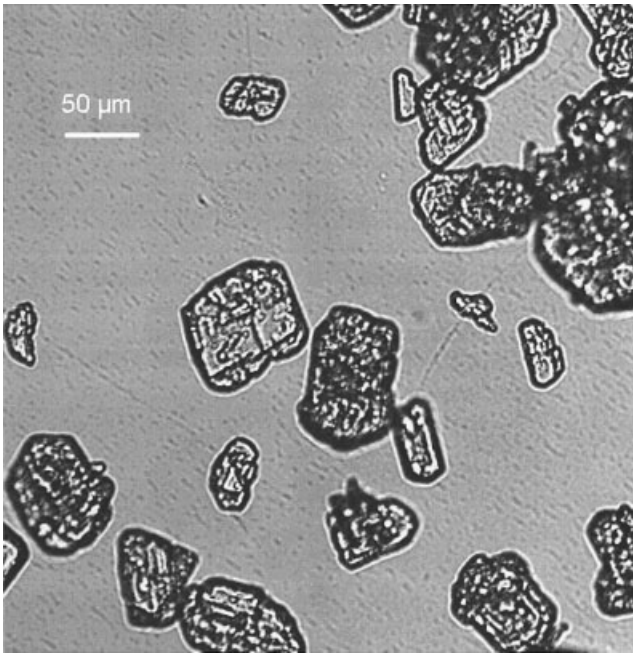

Figure 5. Microscopic image of the D-phenylglycine crystals used in the experiments.

mechanisms by which displacement can occur is through stress applied on the particle by a coinciding eddy or through periodical contraction and elongation of the interface in case the drop oscillates (Schulze, 1984). If, in one of these ways, the kinetic energy gained by the particle exceeds the energy required for desorption ($-\Delta E_{ads}$), the particle can get resuspended into the bulk phase. The kinetic energy that is gained by the particle depends on the intensity of the event and will be distributed around some average value $\Delta E_{kin,0}$, which is specific for the process conditions and the concerned mechanism of desorption. The probability of desorption $P_{des,A}$ can now be expressed as a function of the ratio between ΔE_{ads} and $\Delta E_{kin,0}$, where $P_{des,A}$ approaches unity for $\Delta E_{kin,0}/\Delta E_{ads} \rightarrow \infty$ and $P_{des,A}$ approaches zero for $\Delta E_{kin,0}/\Delta E_{ads} \rightarrow 0$. In this way, the link between the interfacial adsorption energy ΔE_{ads} and the desorption rate can be expressed.

At steady state, the rate of adsorption (viz. Eq. 9a,b) is equal to the rate of desorption (viz. Eq. 12a and 12b). Inspection of Eqs. 9a and 9b, and12a and 12b, reveals that they have a very common form which is often encountered in physical adsorption processes. It can be shown that equating 9a and 9b with 12a and 12b gives upon rearrangement (Campbell, 1988)

$$\theta_A = \frac{\zeta_A c_A}{1 + \zeta_A c_A + \zeta_B c_B} \tag{14a}$$

$$\theta_B = \frac{\zeta_B c_B}{1 + \zeta_A c_A + \zeta_B c_B} \tag{14b}$$

where ζ_A and ζ_B are equal to $k_{ads,A}/k_{des,A}$ and $k_{ads,B}/k_{des,B}$ respectively.

These equations are in essence equivalent to the common Langmuir-isotherms for two species A and B.

With the Langmuir-type model for interfacial partitioning that is formed by Eqs. 14a and 14b, the distribution of particles A and B over the interface and continuous phase can be described in terms of interfacial coverages (θ_A and θ_B) and bulk concentrations (c_A and c_B). For comparison with experimental data, however, it is more convenient to use expressions based on masses of particles. The mass fraction of particles A and B that end up in the interphase is calculated according to

$$f_A = \frac{m_{A,i}}{m_{A,i} + m_{A,s}} = \frac{n_{A,i}}{n_{A,i} + n_{A,s}} = \frac{\theta_A \cdot A_{tot}/a_A}{\theta_A \cdot A_{tot}/a_A + V \cdot c_A} \tag{15a}$$

$$f_B = \frac{m_{B,i}}{m_{B,i} + m_{B,s}} = \frac{n_{B,i}}{n_{B,i} + n_{B,s}} = \frac{\theta_B \cdot A_{tot}/a_B}{\theta_B \cdot A_{tot}/a_B + V \cdot c_B} \tag{15b}$$

Where n is the number of particles, and m represents the mass of particles (kg). Subscripts i and s refer to the interphase and the sediment (that is, continuous phase), respectively.

The degree of separation can now be expressed with a selectivity factor α defined as

$$\alpha = \frac{f_A/(1 - f_A)}{f_B/(1 - f_B)} \tag{16}$$

With Eq. 15a and 15b, it follows that

$$\alpha = \frac{f_A/(1 - f_A)}{f_B/(1 - f_B)} = \frac{m_{A,i}/m_{A,s}}{m_{B,i}/m_{B,s}} = \frac{n_{A,i}/n_{A,s}}{n_{B,i}/n_{B,s}} = \frac{\theta_A \cdot \dfrac{A_{tot}}{a_A} \Big/ (V \cdot c_A)}{\theta_B \cdot \dfrac{A_{tot}}{a_B} \Big/ (V \cdot c_B)} = \frac{\theta_A/c_A}{\theta_B/c_B} \cdot \frac{a_B}{a_A} \tag{17}$$

With 14a and 14b, it can be shown that

$$\frac{\theta_A/c_A}{\theta_B/c_B} = \frac{\zeta_A/(1 + \zeta_A c_A + \zeta_B c_B)}{\zeta_B/(1 + \zeta_A c_A + \zeta_B c_B)} = \frac{\zeta_A}{\zeta_B} \tag{18}$$

Substitution of Eq. 18 into Eq. 17 gives

$$\alpha = \frac{\theta_A/c_A}{\theta_B/c_B} \cdot \frac{a_B}{a_A} = \frac{\zeta_A a_B}{\zeta_B a_A} \tag{19}$$

This equation makes clear that the model predicts a constant selectivity when all four parameters a_A, a_B, ζ_A and ζ_B are assumed to be constants.

Materials and Methods

Crystals and image analysis

Ampicillin trihydrate and D-phenylglycine crystals were used as model particles in this study. Both the ampicillin trihydrate crystals (purity $>$ 99%) and the D-phenylglycine crystals (purity = 96.2%; 92% of impurity being L-phenylglycine) were obtained from DSM (Geleen, The Netherlands). (Ampicillin trihydrate and D-phenylglycine are the full and correct names for the crystals used in this study. For reasons of convenience, these crystals will be referred to simply as ampicillin and phenylgycine throughout the rest of the text). The ampicillin crystals had a rod-like shape with a number averaged length of 6.5 $\pm$ 0.5 μm and a number averaged width of 2.3 $\pm$ 0.2 μm. The phenylglycine crystals had a more compact cubic-like shape with a number averaged diameter of 62 $\pm$ 3 μm. Figures 4 and 5 show pictures of both crystal types obtained with an Olympus IMT2 optical microscope. Shape and size measurements were carried out with Leica Q win V 2.5 Q win pro image analysis software.

Image analysis was applied in order to determine the area effectively covered by 1 g of crystals. For the phenylglycine crystals a total number of 298 crystals was considered. For each crystal the equivalent diameter (being the diameter of the sphere for which the cross sectional area is equal to the area of the crystal's image) was determined. The total mass of the crystals was approximated as the density times the total volume of the spheres with equivalent diameters. The average mass per crystal was then calculated by dividing this value by the number of crystals. The total area covered by the crystals was determined by summing the areas of the crystal images. The value of a_{PG} then followed from dividing this total area by the number of crystals.

For the ampicillin crystals, a total number of 421 crystals were considered. For the determination of the total volume, it was assumed that the crystals were shaped like bars with dimensions L$\times$A$\times$A, where the image showed the bars lying flat on one of the planes with length L and width A. The assumption that the crystals could be regarded as bars was made on the basis of SEM images of ampicillin trihydrate crystals obtained by Ottens et al. (2001) which clearly display the three-dimensional (3-D) shape of the crystals. The average mass per crystal now followed from multiplying with the density and dividing by the number of crystals considered. The total area covered by the crystals was directly determined from the images by summing all projected crystal areas. The value of a_{AMPI} then followed from dividing this total area by the number of crystals considered.

Preparation of liquid biphasic systems

Water was purified with a Milli-Q® water purification system of Waters-Millipore (Milford, MA, USA). n-Pentane of analytical quality was purchased from Mallinckrodt Baker BV (Deventer, The Netherlands). Diethyl ether (99.8%) and 1-hexanol (98%) were obtained from Fluka (Zwijndrecht, The Netherlands). 1-Butanol (99%) was supplied by Acros Organics (Geel, Belgium).

The water/n-pentane systems that were used in the partition experiments were prepared by mixing water with n-pentane together with excess amounts of ampicillin and phenylglycine crystals for about 4 h at room-temperature. Thereafter, the remaining ampicillin and phenylglycine crystals that did not dissolve were separated from the water and organic phase by filtering the liquids with a sterile 0.45 μm filter.

Partition experiments

Partition experiments with the water/n-pentane system were carried out in a cylindrical 200 mL separatory funnel. To the funnel ampicillin and phenylglycine crystals were added, followed by the addition of 66 mL of water phase. The system was then stirred with a stainless steel two-bladed paddle stirrer with a diameter of 29 mm for approximately 1 min to make sure that the crystals were fully dispersed in the water phase. After mixing was stopped, 25 mL of n-pentane phase was added to the system. The system was then stirred for 5 min with a constant rotational speed. The stirrer was positioned such that the blade was immersed in the water phase. This way it was ensured that the n-pentane phase would become the dispersed phase, because under these circumstances, the n-pentane gets sucked into the vortex created by the stirrer and becomes dispersed into droplets in the water phase. The rotational speed was maintained constant at 750 rpm. Tests with pure water/n-pentane systems (without crystals) made clear that this speed was sufficient to disperse the n-pentane phase entirely. After mixing, the continuous water phase with crystals was separated from the interphase layer. Both the water phase and the interphase layer were filtered with a filter paper. The crystals were dried on the filter in an oven at 40°C for 24 h. The dried residues were weighed and dissolved in water. The solutions were analyzed for ampicillin and phenylglycine with HPLC. The mass fraction of phenylglycine crystals X_{PG} in the samples was calculated from the analysis data according to

$$X_{PG} = \frac{m_{PG}}{m_{PG} + m_{AMPI}} \tag{20}$$

where m_{PG} and m_{AMPI} are the masses of phenylglycine and ampicillin crystals in the residue (kg). Furthermore, the analysis data was used to calculate the fractions of ampicillin and phenylglycine in the interphase (f_{AMPI} and f_{PG}).

A small number of partition experiments was carried out on a smaller scale. In this case 2 mL of water and 1 mL of n-pentane, diethyl ether, 1-butanol, or 1-hexanol were added to a test tube. The content of the test tube was mixed with an IKA MS2 minishaker at 1,800 rpm for 20 s. Thereafter, approxi-

Table 1. Partition Data of Ampicillin Trihydrate and D-Phenylglycine Crystals in Different Water/Organic Systems

	Water/n-pentane	Water/diethylether	Water/1-hexanol	Water/1-butanol
Interfacial tension γ_{AB}	50 mN/m*	10.7 mN/m†	8.2 mN/m‡	1.58 mN/m§
$\gamma_{AB} \cdot a_{PG}$	$2 \cdot 10^{-10}$ J	$5.1 \cdot 10^{-11}$ J	$3.9 \cdot 10^{-11}$ J	$7.6 \cdot 10^{-12}$ J
$\gamma_{AB} \cdot a_{AMPI}$	$8 \cdot 10^{-13}$ J	$1.7 \cdot 10^{-13}$ J	$1.3 \cdot 10^{-13}$ J	$2.5 \cdot 10^{-14}$ J
$X_{PG,i}$	0.48	0.92	0.82	0.62
$X_{PG,s}$	0.46	0.005	0.04	0.11
Estimated mass of crystals in interphase m_i	—	26 mg	26 mg	33 mg
Estimated mass of crystals in sediment m_s	—	16 mg	17 mg	10 mg
$\alpha = \frac{f_{PG}/(1-f_{PG})}{f_{AMPI}/(1-f_{AMPI})}$	1	$2 \cdot 10^3$	$1 \cdot 10^2$	13

In each experiment, the mass of phenylglycine and ampicillin crystals was equal. The estimated mass of crystals in interphase and sediment followed from $X_{PG,i}$ and $X_{PG,s}$ by making a mass balance for the phenylglycine and ampicillin crystals. Account was taken of the fact that part of the initially added crystals would dissolve. For further details the reader is referred to earlier work (Jauregi et al., 2001).
*: Estimated interfacial tension obtained from extrapolation of data for n-hexane, n-heptane and n-octane.
†: Weast et al. (1922).
‡: Jufu et al. (1986).
§: Janssen and Warmoeskerken (1987).

mately 30 mg of phenylglycine and ampicillin crystals were added to the system, and the test tube was mixed again for 30 s. The test tube was then put aside to allow the formation of the interphase layer and sediment. Samples were taken from the interphase layer and the sediment with a Pasteur pipette and dissolved in water. The ampicillin and phenylglycine content of the samples was analyzed with HPLC.

HPLC analysis

The ampicillin and phenylglycine concentrations of the samples were analyzed with a Waters 2690 HPLC Separation module and a Waters 486 tuneable absorbance detector. The components were separated on a Hewlett-Packard Zorbax SB-C18 column, with an internal diameter of 4.6 mm and a length of 7.5 cm. The particle diameter of the column material was 3.5 μm. Isocratic elution with a buffer consisting of water (80 vol %), methanol (20 vol %), $NaH_2PO_4 \cdot H_2O$ (9.6 g/L) and 85 wt % phosphoric acid solution (0.5 mL/L) was employed. The flow rate was equal to 1 mL/min. Peaks were detected by UV absorption at a wavelength of 210 nm.

Results and Discussion

Interfacial partitioning behavior in different biphasic systems

Table 1 shows the results of small scale interfacial partitioning experiments with several liquid biphasic systems. The data in Table 1 show that in each system the mass fraction phenylglycine in the interphase is higher than in the sediment ($X_{PG,i} > X_{PG,s}$), which indicates that in all cases the interphase is enriched with phenylglycine, and the sediment is enriched with ampicillin. The efficiency of the separation, however, varies considerably with the biphasic systems. Water/diethyl ether and water/n-pentane can be considered to be the extreme cases with the water/diethyl ether system featuring a high degree of separation, and the water/n-pentane system giving an interphase and a sediment with almost equal crystal compositions. In the bottom row of Table 1, the selectivity α, according to Eq. 16, is listed.

A pronounced variation in α with the biphasic systems can be observed. Taking the interfacial tensions of the systems in consideration, it learns that there seems to be an optimum in case the interfacial tension is somewhere between the values for water/butanol and water/n-pentane. The interfacial tension has a direct influence on the adsorption energy ΔE_{ads}, which for a spherical particle is described by Eq. 6. For an arbitrarily shaped particle, the following general equation holds

$$\Delta E_{ads} = \Delta A_{AB}\gamma_{AB} + \Delta A_{AS}\gamma_{AS} - \Delta A_{AS}\gamma_{BS} \qquad (21)$$

where ΔA_{AS} = the change in the interfacial area between the solid and liquid A, in which the particle is fully immersed before adsorption.

The first term on the righthand side of Eq. 21, represents the energetically favorable effect of reduction of the liquid-liquid interfacial area. Its magnitude is, therefore, an indication of the driving force for interfacial adsorption. In Table 1, $a_{PG} \cdot \gamma_{AB}$ and $a_{AMPI} \cdot \gamma_{AB}$, which can be seen as the maximum values of $\Delta A_{AB} \cdot \gamma_{AB}$ per crystal, are given. All values of $a_{PG} \cdot \gamma_{AB}$ and $a_{AMPI} \cdot \gamma_{AB}$ listed in Table 1 are several orders of magnitude larger than kT ($= 4 \cdot 10^{-21}$ J) and ΔE_g, which is $3.2 \cdot 10^{-15}$ J for a phenylglycine crystal of average dimensions, and $1.6 \cdot 10^{-20}$ J for an ampicillin crystal of average dimensions (assuming a flat orientation on the interface). This indicates that, unless there is a large difference between γ_{AS} and γ_{BS}, both phenylglycine and ampicillin show the tendency to adsorb at the interface. An explanation for the observed behavior in terms of differences in interfacial adsorption of the two crystals can therefore only be found if the affinity between solid and liquids (that is, γ_{AS} and γ_{BS}) are taken into consideration.

The interfacial tension can be considered to be a measure for the affinity between the water and the organic phase. A high value of the interfacial tension implies a high degree of hydrophobicity of the organic phase. The relatively low value of α for the water/n-pentane system can be explained by a high hydrophobicity of the organic phase. Both crystals consist of molecules that contain polar groups, and it seems plausible that because of n-pentane's high hydrophobicity, the crystals do not partition into the n-pentane phase and adsorb only moderately at the interface. The selectivity now results from a difference in

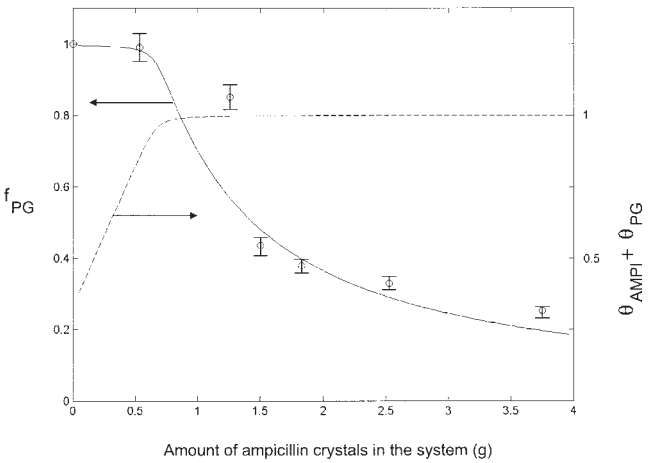

Figure 6. Fraction of phenylglycine crystals that partition to the interphase vs. the amount of ampicillin crystals added to the system.

The data was obtained from experiments in water/n-pentane systems with a constant amount of 2.5 g of phenylglycine. Each data point represents the result of a single experiment. The reproducibility of the experiments was not assessed. The error bars indicate the 95% confidence interval of the analysis method. The curve was obtained with the model after fitting to the data points in Figures 6 to 9.

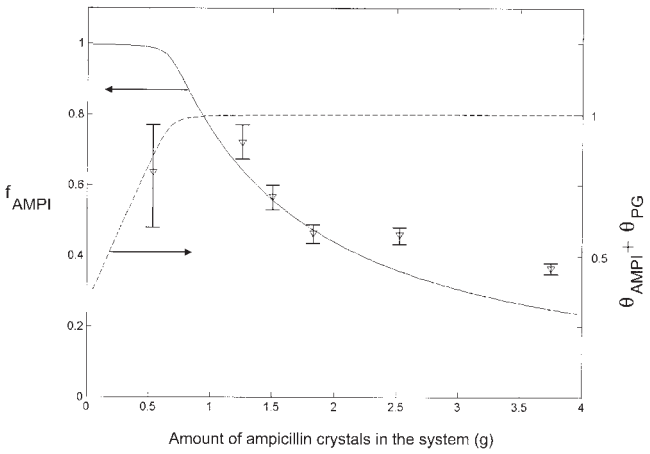

Figure 7. Fraction of ampicillin crystals that partition to the interphase vs. the amount of phenylglycine crystals added to the system.

The data was obtained from experiments in water/n-pentane systems with a constant amount of 2.5 g of ampicillin. Each data point represents the result of a single experiment. The reproducibility of the experiments was not assessed. The error bars indicate the 95% confidence interval of the analysis method. The curve was obtained with the model after fitting to the data points in Figures 6 to 9.

the degree of adsorption of the two types of crystals at the droplets.

This is probably different with the other three systems. Here, the organic phases are much more polar, and it seems reasonable to assume that part of the crystals can actually end up inside it. Particles that reside in the organic phase will either find themselves inside the droplets in the interphase, or lie on top of this layer and will either way be collected with the interphase layer. The very high degree of separation in the water/diethyl ether system might now be explained by assuming that the diethyl ether phase is still too apolar to have ampicillin partition into it, but polar enough to fully wet phenylglycine. This results in a high selectivity. In comparison, the organic phases in the water/butanol and water/hexanol systems are much more polar, and here ampicillin might end up in the organic phase as well.

The results in Table 1 show clearly that interfacial partitioning as a single-step separation of particle mixtures can already lead to a high selectivity. Especially the results with the water/diethyl ether and the water/hexanol system seem promising for the underlying model system. As mentioned previously, in these systems it is likely that phenylglycine partly ends up in the organic phase. Crystals that sediment in the organic top phase are collected together with the interphase, and it is therefore impossible to distinguish them from crystals that are adsorbed at the interfaces of the droplets. This means that the water/diethyl ether and water/hexanol systems are unsuitable for a mechanistic study on the distribution of particles between the interface and continuous phase. This is probably not the case for the water/n-pentane system, where partitioning into the n-pentane phase most likely does not occur. In the following, water/n-pentane will therefore be used for a mechanistic study of the partition mechanism.

Interfacial partitioning behavior of ampicillin and phenylglycine in a water/n-pentane system

The results of the partition experiments carried out with water/n-pentane systems are shown in Figures 6 – 9. The data points in both Figures 6 and 7 were obtained from the same set of experiments and display the effect of the addition of ampicillin crystals at a constant amount of phenylglycine crystals on the partitioning of phenylglycine and ampicillin. Likewise, Figures 8 and 9 show the influence of various amounts of

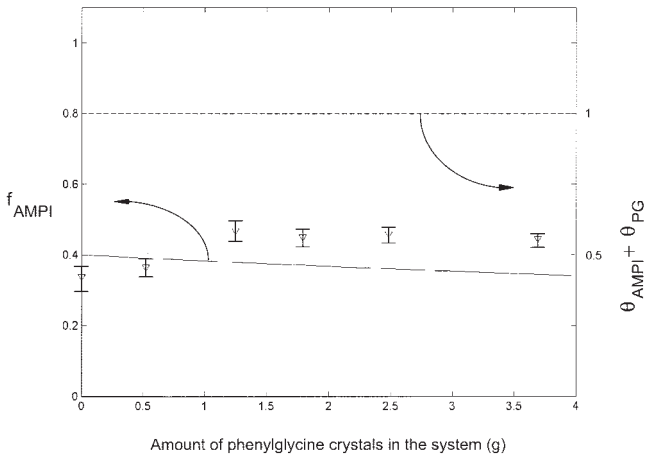

Figure 8. Fraction of ampicillin crystals that partition to the interphase vs. the amount of ampicillin crystals added to the system.

The data was obtained from experiments in water/n-pentane systems with a constant amount of 2.5 g of phenylglycine. The error bars indicate the 95% confidence interval of the analysis method. The curve was obtained with the model after fitting to the data in Figures 6 to 9. The dashed line shows the interfacial coverage of the droplets as calculated with the model.

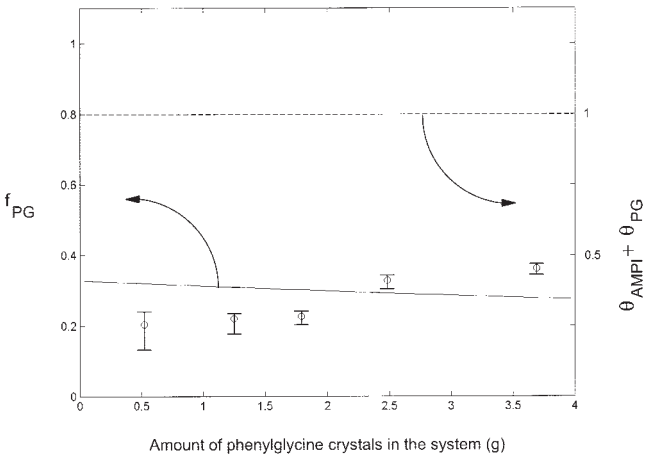

Figure 9. Fraction of phenylglycine crystals that partition to the interphase vs. the amount of phenylglycine crystals added to the system.

The data was obtained from experiments in water/n-pentane systems with a constant amount of 2.5 g of ampicillin. The error bars indicate the 95% confidence interval of the analysis method. The curve was obtained with the model after fitting to the data in Figures 6 to 9. The dashed line shows the interfacial coverage of the droplets as calculated with the model.

phenylglycine crystals at constant loading of ampicillin. The curves were calculated with the model presented in the theory section and will be further discussed later.

Low crystal loading

The results in Figure 6 show a very markedly effect of the addition of ampicillin on the partition behavior of phenylglycine. When the loading of ampicillin is increased to values above 1 g, the fraction of phenylglycine crystals that ends up in the interphase (f_{PG}) drops suddenly from 1 to values below 0.5. This indicates that there seems to be a distinctive value for the ampicillin loading where the capacity of the interphase for phenylglycine is reached. Most probably this corresponds to the point where the interfaces of the droplets are just entirely covered by the crystals. The fact that f_{PG} is close to unity at low loadings indicates that for the phenylglycine crystals the tendency to adsorb and to stay adsorbed at the droplets is large. In Figure 7 it can be seen that this does not seem to be the case for the ampicillin crystals. The data points show that, at a loading of about 0.5 g, the value of f_{AMPI} is only slightly higher than 0.6. Apparently the adsorption of ampicillin is not complete at low loadings. It seems that under these conditions the ampicillin crystals do not adsorb as strongly as the phenylglycine crystals, and a dynamic equilibrium is reached between adsorption and desorption of ampicillin crystals.

High crystal loading

The sudden drop in f_{PG} in Figure 6 indicates that once the loading with crystals in the system reaches a certain critical value, the phenylglycine crystals start to sediment in the continuous water phase. It is probable that this critical value marks the point at which the available interface is entirely covered with crystals. The addition of more ampicillin leads to a displacement of phenylglycine from the interface. At the same time it is expected that also f_{AMPI} will drop at some stage as there is – of course – a limit to the amount of ampicillin crystals that fit on the surface of the drops. Although not as pronounced as is the case for f_{PG}, a decreasing trend in f_{AMPI} can indeed be observed for loadings above 1 g (Figure 7). So with these loadings, both ampicillin and phenylglycine partition to the continuous water phase. The distribution of the crystals over interphase and sediment and, therefore, also the degree of separation is now determined by a competition for the interfacial area.

The data in Figure 8 and 9 show the effect of the addition of phenylglycine at a constant loading of 2.5 g of ampicillin. In each of these experiments the amount of ampicillin crystals was already sufficient to entirely cover the drops (see under the section *Estimation of model parameters*), and as such it is expected that competition for the interfacial area occurred here. The data show that f_{AMPI} assumes a more or less constant value close to 0.4, whereas f_{PG} fluctuates about a somewhat lower value of around 0.3. What is remarkable is the absence of a decreasing trend in f_{PG} and f_{AMPI}. Apparently, here, no significant exclusion of crystals from the droplet interfaces seems to occur as the loading is increased to up to 4 g. The absence of an exclusion effect might be explained by the relatively large size of the phenylglycine crystals. The large diameter implicates that the crystals have a small area to volume ratio. Therefore, the addition of up to 4 g of phenylglycine crystals extra might not have a large impact on the total interfacial area that is being covered, (as opposed to the effect that was observed with the much smaller ampicillin crystals).

Estimation of model parameters

The results in Figures 6 to 9 indicate that there is clearly a limit to the amount of crystals that can be adsorbed at the drops, which means that competition for the interfacial area should occur at high loadings. The maximum loading of crystals on the drops is determined by the available interfacial area A_{tot} and the number-averaged area covered per crystal (a_{PG} or a_{AMPI}). The values of a_{PG} and a_{AMPI} were determined with image analysis to be 4,800 μm^2 and 15.7 μm^2, respectively. Multiplying these values with the average mass per crystal gives the area covered per unit mass of crystals. In this way it is found that the values above correspond to 0.02 m^2 per g of phenylglycine crystals and 0.15 m^2/g for ampicillin. A_{tot} is directly related to the drop-size distribution and the total volume of dispersed phase in the particles-containing system. An estimation of the average drop diameter was, however, obtained from experiments with the water/n-pentane system without particles. A reliable measurement was not possible, but the average diameter d_d of the n-pentane drops in the creamed emulsion layer just after stirring was estimated to be around 1 ± 0.5 mm. The total interfacial area A_{tot} for a total dispersed phase volume V_d can then be calculated with $A_{tot} = 6 \cdot V_d / d_d$, which gives for 25 mL of dispersed phase $A_{tot} = 0.15$ m^2. Hence, the amount of crystals needed to cover the drops entirely is 0.15/0.15 = 1 g for ampicillin, and 0.15/0.02 = 7.5 g for phenylglycine. The value of 1 g for ampicillin is in good correspondence with the observed decrease in f_{PG} somewhere in the range of 1–1.5 g in Figure 6. The estimated values A_{tot}, a_{AMPI} and a_{PG} can directly be used in the model.

Further parameters that occur in the model are the kinetic

rate ratios ζ_{AMPI} and ζ_{PG}. Prediction of these values requires detailed knowledge of the mechanism of adsorption and desorption of the particles. At this stage, however, our knowledge about these mechanisms is insufficient to enable a reasonable quantitative prediction of ζ_{AMPI} and ζ_{PG}.

Evaluation of the model

The curves in Figures 6 to 9 show the partition data for ampicillin and phenylglycine calculated with the model. The estimations for A_{tot}, a_{AMPI} and a_{PG} given earlier were used as parameters in the model, and ζ_{AMPI} and ζ_{PG} were obtained by fitting. For the determination of the best fit, the least sum of squares method was employed, using all data in Figures 6 to 9. In Figure 6, it can be seen that the drop in f_{PG} somewhere in the range of 1 – 1.5 g is reasonably predicted with the model. The curve shows a slight underestimation of the point where f_{PG} drops, but this is most likely well within the limits of accuracy considering the uncertainty in the estimations of a_{AMPI}, a_{PG} and A_{tot}. From the plotted value of $\theta_{PG} + \theta_{AMPI}$, it is clear that the sharp drop in f_{PG} occurs when total coverage of the drops is reached, because $\theta_{AMPI} + \theta_{PG}$ reaches the value of 1 at this point.

The prediction of the partition data for ampicillin in Figure 7 seems to be less accurate. Although the description of the decrease in f_{AMPI} at higher loadings is fair, the model fails to predict the low value of about 0.63 at a loading of 0.5 g of ampicillin. In this particular experiment, the amount of crystals in the system was relatively low. The fraction of the interfacial area that could be covered by them (assuming complete adsorption) can be estimated on the basis of a_{AMPI}, a_{PG} and A_{tot} to be only 65%. This means that the droplets could not have been totally covered with crystals yet at this point. It is imaginable that under these conditions the kinetics of the partition mechanism differ from situations with a high or complete coverage of the droplets. Perhaps at high interfacial coverages, the ampicillin crystals are more firmly positioned because of the formation of a tight 2-D packing of particles. Once an ampicillin crystal adsorbs, it might get fixed rather easily between neighboring particles because of its rod-like shape. At low coverages, however, desorption of crystals from the droplets might occur more easily, leading to an unexpectedly low value of f_{AMPI}.

Another explanation for the low value of f_{AMPI} at low loading might be related to the broad-size distribution. It is likely that the partition behavior of the crystals is dependent on size. First, there is an influence of the size on the adsorption energy ΔE_{ads}. The measured-size distribution is such that 90 wt % of the ampicillin crystals has a length between 6 and 22 μm, and a width between 2 and 6 μm. Within this size range, the interfacial forces are generally still much more important than gravity. However, if the contact angle ϕ_{eq} is very small, there is still a possibility that some of the (larger) ampicillin crystals are less firmly attached than the rest. Furthermore, the particle size will have an effect on the kinetics of the process on hydrodynamic grounds. The process of thinning of the liquid film between drop and particle, for example, is highly dependent on particle size. In view of this, it is plausible that the size distribution of the crystals is so broad that the partition behavior of the crystals ranges from "strongly adsorbing" to "virtually nonadsorbing". The ampicillin crystals that do adsorb at the interface, might bind strong enough to be able to exclude phenylglycine crystals from adsorption. This could explain why phenylglycine gets excluded from the interface by ampicillin even though there is always a fraction of ampicillin crystals that does not adsorb.

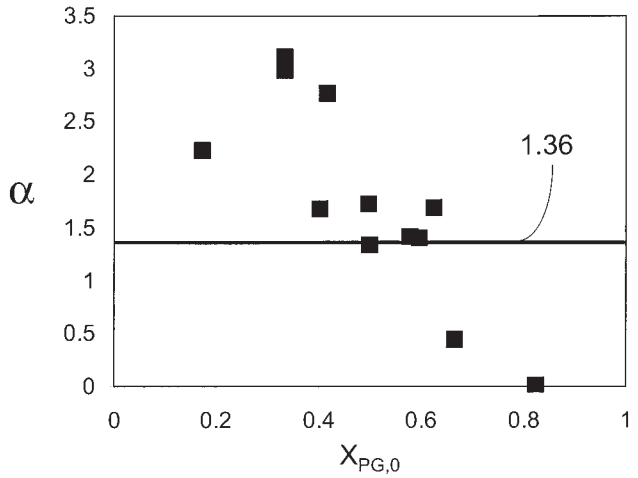

Figure 10. The selectivity plotted vs. the mass fraction of phenylglycine crystals in the crystal mixture added to the funnel.

The definition of α reads: $(f_{AMPI}/(1- f_{AMPI}))/(f_{PG}/(1- f_{PG}))$. Note that this definition is the reciprocal of the one used in Table I. The horizontal line shows the value of the selectivity that was calculated from the fit parameters in the model after fitting the data in Figures 6 to 9.

Figures 8 and 9 show that the model predicts a small decreasing trend in f_{AMPI} and f_{PG} with an increased amount of phenylglycine crystals. However, there appears to be an upward rather than a downward trend in the experimental data of f_{AMPI} and f_{PG}. This means that apparently more crystals adsorb at the droplets when higher loadings are used. This could indicate that there is an increase in interfacial area with the amount of phenylglycine crystals. Similar effects were reported by Ashby and Binks (2000) who showed that Laponite clay particles can cause a decline of the drop diameter (and, hence, an increase in interfacial area) in toluene-in-water emulsions. Effects like these are particularly hard to predict quantitatively and were not considered in the model. Incorporation of this phenomenon is expected to improve the model further. However, the effect seems to be limited and considering the accuracy of the experimental data, it can be argued that this model gives a reasonable first-order description of the partition behavior at varying loading of phenylglycine.

In Figure 10 the selectivity is plotted vs. the mass fraction of ampicillin $X_{PG,0}$ in the crystal mixture added to the funnel. The model is based on the assumption of constant kinetic rate ratios ζ_{PG} and ζ_{AMPI} and, hence, a constant selectivity for the two components. The horizontal line in the graph indicates a selectivity value of 1.36, which was calculated with the previously obtained fit parameters. The data points are more or less scattered around 1.36, but it would be rather unrealistic to suggest that the selectivity is constant. There are even two data points with a value below 1, which means that at some point the selectivity is inverted. Inspection of all data gives the impression that there is an almost linear trend downward in α.

At this point we have no explanation for this fact, but it is not unlikely that this should be labeled as an artefact. Nevertheless, it remains clear that the assumption of constant kinetic rate ratios ζ_{AMPI} and ζ_{PG} does not hold for the whole range of this set of data. This illustrates the need for a more fundamental theoretical understanding of the mechanisms of adsorption and desorption which determine these parameters. A better understanding of these mechanisms could clarify under which conditions the assumption of constant selectivity applies.

Conclusions

Interfacial partitioning experiments with ampicillin and phenylglycine crystals in different water/organic two-phase systems showed that the degree of separation is largely dependent on the choice of the organic phase. The best results were obtained when the polarity of the organic phase was moderate. Most likely this is the result of phenylglycine crystals partitioning to the organic phase (apart from adsorbing at the interface), whereas the more polar ampicillin crystals predominantly partitioned to the water phase. It was shown that the selectivity of a one-step process can be very high in this case.

A water/n-pentane system was used to study the partition behavior of the crystal mixture between interface and continuous water phase. It was shown that the partition data can be reasonably described with a Langmuir-type model based on the competitive adsorption of the particles at dispersed phase droplets. Predictions of model parameters concerning the capacity of the droplets could be reasonably made on the basis of the crystal-size distribution, and an estimation of the drop size. The experimental data indicated a clear distinction between situations of high and low-loading of the droplets. At high loading, a mechanism of competitive adsorption applies and an exclusion of crystals from the interface was observed. At low loading, the coverage of the interface by crystals is incomplete, and the interaction between the particles is limited. The experimental results indicated that the partition behavior of the crystals can differ considerably under these conditions, leading to variations in selectivity. In its current state, the model does not allow for variation of the selectivity and a more fundamental understanding of the mechanisms of adsorption and desorption of the particles is needed to incorporate this.

Acknowledgments

The authors would like to acknowledge DSM's financial support. The authors also acknowledge the financial support of the Dutch Ministries of Economic Affairs, Education and Agriculture in their combined ABON programme for the stimulation of integrated bioprocess development. We also thank Marijn Rijkers and Pim van Hee for their contribution to the discussions for this article and Stef van Hateren for his collaboration with the image analysis of the crystals.

Notation

a_A, a_B ... = the interfacial area that a single particle effectively covers, m^2
ΔA_{AB} = the change in area of a liquid-liquid interface because of the presence of a particle, m^2
ΔA_{AS} = the change in interfacial area between the solid and liquid A, in which the particle is fully immersed before adsorption, m^2
A_{tot} = the total droplet interfacial area, m^2
c = the number concentration of particles, m^{-3}
d_d = the average drop size, m
d_p = the diameter of a spherical particle, m
ΔE_{ads} = the energy required to remove a particle from the interface into the bulk liquid phase, J
ΔE_g = the change in gravitational energy as a particle moves in the direction of the net force, that arises from gravity and buoyancy, over a distance of half its diameter, J
$\Delta E_{kin,0}$ = the average kinetic energy of a particle (relative to the interface) during a desorption event, J
f_{AMPI}, f_{PG} = the fraction of ampicillin (phenylglycine) crystals that partition to the interphase
F_g = net resultant of the gravity and buoyancy force, N
g = gravitational acceleration, m/s^2
k = Boltzmann constant= $1.38 \cdot 10^{-23}$ J/K.
k_{ads} = rate constant for the adsorption of particles on droplets, m/s
k_{col} = rate constant for collisions of particles with droplets, m/s
k_{des} = rate constant for the desorption of particles adsorbed at droplets, $m^{-2}s^{-1}$
k_{freq} = rate constant indicating the frequency of events that can possibly result in desorption of particles from droplets, $m^{-2}s^{-1}$
m = the mass of particles, kg
n = the number of particles
P_{des} = the probability that desorption of a particle from the interface actually does occur
P_{int} = the probability that the thin liquid film between particle and droplet will rupture
P_{hyd} = the hydrodynamic capture probability
P_{TPC} = the probability of a successful three-phase contact formation
r_{ads} = the number of effective collisions between particles and droplets per unit of time and unit of volume, $m^{-3}s^{-1}$
r_{des} = the desorption rate for particles adsorbed at droplets, $m^{-3}s^{-1}$
T = the absolute temperature, K
V = the total volume of the continuous phase, m^3
V_d = the total dispersed phase volume, m^3
X_{AMPI}, X_{PG} = the mass fraction of ampicillin (phenylglycine) crystals in a crystal mixture

Greek letters

α = selectivity
γ_{AS}, γ_{BS}, γ_{AB} = interfacial tension at the AS, BS, or AB interface, N/m
ϕ = the contact angle between the liquid-liquid interface and the solid-liquid interface
ϕ_{eq} = the equilibrium contact angle for a sphere residing at the liquid-liquid interface
θ_A, θ_B = the fraction of droplet interface covered with particles A or B
ρ_p = the density of the particle, kg/m^3
$\bar{\rho}$ = the average density of the liquid phases (kg/m^3).
ζ_A, ζ_B = kinetic rate ratios for particles A and B that partition between droplet interface and continuous liquid phase, m^3

Subscripts

A = particle A
$AMPI$ = ampicillin
B = particle B
i = interface or interphase
PG = phenylglycine
s = sediment

Literature Cited

Andrews, B. A., R. B. Huang and J. A. Asenjo, "Purification of Virus like Particles from Yeast Cells using Aqueous Two-Phase Systems," *Bioseparation*, **5**, 105 (1995).
Ashby, N. P., and B. P. Binks, "Pickering Emulsions Stabilised by Laponite Clay Particles," *Phys. Chem. Chem. Phys.*, **2**, 5640 (2000).
Binks, B. P., and S. O. Lumsdon, "Stability of Oil-In-Water Emulsions

Stabilised by Silica Particles," *Phys. Chem. Chem. Phys.*, **1**, 3007 (1999).
Binks, B. P., and S. O. Lumsdon, "Influence of Particle Wettability on the Type and Stability of Surfactant-Free Emulsions," *Langmuir*, **16**, 8622 (2000a).
Binks, B. P., and S. O. Lumsdon, "Transitional Phase Inversion of Solid-Stabilized Emulsions Using Particle Mixtures," *Langmuir*, **16**, 3748 (2000b).
Binks, B. P., and S. O. Lumsdon, "Effects of Oil Type and Aqueous Phase Composition on Oil-Water Mixtures Containing Particles of Intermediate Hydrophobicity," *Phys. Chem. Chem. Phys.*, **2**, 2959 (2000c).
Binks, B. P., and S. O. Lumsdon, "Catastrophic Inversion of Water-In-Oil Emulsions Stabilized by Hydrophobic Silica," *Langmuir*, **16**, 2539 (2000d).
Bruggink, A., E. C. Roos, and E. Vroom, "Penicillin Acylase in the Industrial Production of β-lactam Antibiotics," *Org. Process Res. Dev.*, **2**, 128 (1998).
Campbell, I. M., *Catalysis at surfaces*, Chapman and Hall, London, (1988)
Dennison, C., and R. Lovrien, "Three Phase Partitioning: Concentration and Purification of Proteins," *Protein Expr. Purif.*, **11**, 149 (1997).
Halling, P. J., U. Eichhorn, P. Kuhl, and H. D. Jakubke, "Thermodynamics of Solid to Solid Conversion and Application to Enzymic Peptide Synthesis," *Enzyme Microb. Technol.*, **17**, 601 (1995).
Janssen, L. P. B. M., and M. M. C. G. Warmoeskerken, *Transport Phenomena Data Companion*, Delftse Uitgevers Maatschappij, Delft (1987).
Jauregi, P., M. A. Hoeben, R. G. J. M. Van der Lans, G. Kwant, and L. A. M. Van der Wielen, "Recovery of Small Bioparticles by Interfacial Partitioning," *Biotechnol. Bioeng.*, **78** (4), 355 (2002).
Jauregi, P., M. A. Hoeben, R. G. J. M. Van der Lans, G. Kwant, and L. A. M. Van der Wielen, "Selective Separation of Physically Near-Identical Microparticle Mixtures by Interfacial Partitioning," *Ind. Eng. Chem. Res.*, **40**, 5815 (2001).
Jufu, F., L. Buqiang, and W. Zihao, "Estimation of Fluid Interfacial Tensions of Multimixtures," *Chem. Eng. Sci.*, **41**, 2673, (1986).
Kimura, K., and H. Kobayashi, "RNA Partitioning Accompanied by Adsorption: High-Molecular-Mass RNA Adsorbed at the Interface like a Particle," *J. Chromatogr. B*, **680**, 213 (1996).
Levine, S., B. D. Bowen, and S. J. Partridge, "Stabilization of Emulsions by Fine Particles I. Partitioning of Particles Between Continuous Phase and Oil/Water Interface," *Colloids Surf.*, **38**, 325 (1989a).
Levine, S., B. D. Bowen, and S. J. Partridge, "Stabilization of Emulsions by Fine Particles II. Capillary and Vanderwaals Forces Between Particles," *Colloids Surf.*, **38**, 345 (1989b).
Liu, B. L., Y. M. Tzeng, and C.T. Wei, "Recovery of Solubilized δ-endotoxin from *Bacillus Thuringiensis* Subsp Kurstaki Fermentation Broth", *Pest Manag. Sci.*, **56**, 448 (2000).
Ottens, M., B. Lebreton, M. Zomerdijk, M. P. W. M. Rijkers, O. S. L. Bruinsma, and L. A. M. Van der Wielen, "Crystallization Kinetics of Ampicillin," *Ind. Eng. Chem. Res.*, **40**, 4821 (2001).
Pickering, S. U., "Emulsions," *J. Chem. Soc. Trans.*, **91**, 2001 (1907).
Pike, R. N., and C. Dennison, "Protein Fractionation by Three Phase Partitioning (TPP) in Aqueous/t-butanol Mixtures," *Biotechnol. Bioeng.*, **33**, 221 (1989).
Schulze, H.J., *Physico-Chemical Elementary Processes in Flotation*, Elsevier, Amsterdam (1984).
Tambe, D. E., and M. M. Sharma, "The Effect of Colloidal Particles on Fluid-Fluid Interfacial Properties and Emulsion Stability," *Adv. Colloid Interface Sci.*, **52**, 1 (1994).
Walker, S. G., and A. Lyddiatt, "Processing of Nanoparticulate Bioproducts: Application and Optimisation of Aqueous Two-Phase Systems," *J. Chem. Technol. Biotechnol.*, **74**, 250 (1999).
Weast, R. C., M. J. Astle, and W. H. Beyer, eds., *CRC Handbook of Chemistry and Physics,* 64th ed., CRC Press, Boca Raton, FL (1922).
Wong, H. H., B. K. O'Neill, and A. P. J. Middelberg, "Centrifugal Recovery and Dissolution of Recombinant Gly-IGF-II Inclusion Bodies: The Impact of Feed Rate and Re-Centrifugation on Protein Yield," *Bioseparation*, **6**, 185 (1996).
Yan, N., and J. H. Masliyah, "Adsorption and Desorption of Clay Particles at the Oil-Water Interface," *J. Colloid Interface Sci.*, **168**, 386 (1994).
Yan, N., and J. H. Masliyah, "Characterization and Demulsification of Solids-Stabilized Oil-in-Water Emulsions Part 1. Partitioning of Clay Particles and Preparation of Emulsions," *Colloids Surf. A*, **96**, 229 (1995).

Manuscript received Jan. 8, 2003, and revision received Sept. 2, 2003